Vol. 41, No. 2 (2019) 172-187, DOI: 10.24874/ti.2019.41.02.04

Tribology in Industry

www.tribology.rs

RESEARCH

# Investigation on Tool Wear and Surface Characteristics in Hard Turning Under Air-Water Jet Spray Impingement Cooling Environment

R. Kumar[a], A.K. Sahoo[a], P.C. Mishra[a], R.K. Das[a]

[a] *School of Mechanical Engineering, KIIT Deemed to be University, Odisha, India.*

Keywords:

*Hard turning*
*Spray impingement cooling*
*Flank wear*
*Surface roughness*
*Surface topology*
*Tool life*
*Cost analysis*

Corresponding author:

*Ramanuj Kumar*
*School of Mechanical Engineering,*
*KIIT Deemed to be University,*
*Bhubaneswar-24, Odisha, India*
*Phone: +06746540805*
*Email: ramanujkumar22@gmail.com*

A B S T R A C T

*Low cost machining puts tremendous pressure on the research in machining hardened steel compared to traditional grinding. As environmental regulations are strict enough on application of cutting fluids, a novel method called spray impingement cooling (SIC) assisted hard turning has been studied. The current work explores the distinguish wear modes, surface characteristics, chip-tool interface temperature and chip morphology in turning of AISI D2 steel by coated carbide tools (TiN/TiCN/$Al_2O_3$/TiN). The results revealed the favorable chip tool interaction during machining in context to surface roughness, surface topology, flank wear, chip morphology, chip reduction coefficient and tool life. In the SIC, evaporation occurred due to atomization of water jet and sufficient to generate significant cooling as maximum temperature has been found as 200.6 $^0$C. Modes of wear like abrasion, chipping and catastrophic breakage are noticed at tool-tip in hard turning. The optimal settings of parameters are founds as $a_{p1}$-$f_{n1}$-$v_{c2}$ i.e.* depth of cut-*0.1 mm; feed-0.04 mm/rev; cutting speed-108 m/min. At these parametric conditions, the measured tool life is found as 20.3 minutes.*



## 1. INTRODUCTION

Hardened steel with hardness beyond to 45 HRC is considered to be difficult to turn. Due to their broad applications in molds and dies making industries, automobile industries, electronic industries etc., various attempts have been made by researchers to investigate their machinability. The cutting tool materials such as ceramic, CBN, coated ceramic and coated CBN performed excellent in hard turning applications and produced closer machinability characteristics to grinding process [1]. Applications of these cutting tools are not economical and hence researchers are now more attracted towards low cost-cutting tool like multicoated carbide tools for machining of hardened steel. The innovation of various coating techniques provides us improved carbide cutting insert like multilayer coated carbide where CVD and PVD methods have been used to deposit layer by layer of different materials on the substrate. The deposition of hard and wear resistant coating layers on the insert start near the beginning 1970s and till date about 80 % inserts used in metal machining

industry are coated cemented carbide grades and mostly inserts are CVD-coated due to its wide application for removing high amounts of material while they retain a longer tool life. Generally, TiCN, $Al_2O_3$, TiN, and $ZrO_2$ are some typical coating materials used as coating layers of different thickness on carbide substrate. Diamond coating on titanium alloy by PVD technique provides superior performance on mechanical properties [2]. It is observed that friction properties of the interfacial layer of TiC composite coating enhanced compared to surface TiC coating [3]. TiCN coating provides very good abrasive wear resistance and good adherence while $Al_2O_3$ ensures very good external thermal and chemical shield for the insert substrate. TiN is widely used for the golden color for visualization of wear detection and provide better wear resistance and lubrication whereas $ZrO_2$ confirms very good thermal and chemical shield for the insert substrate [1,4].

Usually, hard turning has been carried out in the dry scenario but the absence of cutting fluid creates a problem in chip disposal, bring about an elevated temperature at chip- tool interface that leads to diffusion wear and develops the high amount of friction between chip-tool and tool- work that promotes higher abrasion wear. However, the use of abundant coolant is advantageous of chip disposal, reduction of machining region temperature and friction but it increases the cost of machining process as well as injurious to the health of human being. So, in recent years, researchers have been more interested in the use of minimum amount of coolant known as close to dry machining or minimum quantity lubrication (MQL) where mixture of pressurized air and oil are used [5]. Machining under spray impingement cooling is also a kind of near to dry machining where compressed air and water mixture are used.

Principal tool wear mechanism in hard machining using coated carbide tools of multi-layer coating (TiN/TiCN/$Al_2O_3$/TiN) is found to be abrasion and chipping. The feed rate was observed to be the most compelling cutting variable for average surface roughness and flank wear [4, 6]. Cutting performances in spray impingement cooling have been improved compared to the dry turning of hardened AISI 1015 steel (43 ± 1HRC) using carbide tool and the cutting temperature was improving with feed and spindle speed. The optimum result in cooling condition was found with air pressure and water pressure of 1.5 bar & 1 bar respectively [7]. Machining under spray cooling environment produced better surface quality, reduced cutting tool temperature and improved productivity as compared to dry situation owing to decline in friction at cutting zone [8]. D2 steel machining using tungsten carbide insert under near dry environment yielded promising results over dry machining. Compare to dry cutting, the surface integrity was improved and cutting temperature was reduced by almost 50% in near dry machining [9]. The coated carbide tool life was 3.3 times higher than PCBN tool at 60 m/min of rotational speed but at rotational speed 175 m/min, PCBN attained higher tool life relative to coated tungsten carbide due to its greater hot hardness [10]. The average work surface roughness was extremely swayed by the cutting feed succeeded by cutting speed and depth of cut in turning process of hardened alloy steel ( up to 69 HRC) using CBN cutting tools under dry cutting situation [11]. Cutting speed attributed the largest impact on wear caused due to severe abrasion while the depth of cut strongly affected to the forces involved in cutting [12]. The depth of cut and feed were compelling aspects to influence the cutting and radial forces involved in turning of hard to cut material whereas the surface roughness was extremely exaggerated by the depth of cut followed by feed and cutting speed [13]. The most advantageous finish surface was introduced with consideration of smallest feed and largest cutting speed in hard machining [14].

Generation of high cutting temperature in hard turning deteriorates surface quality and accelerates tool wear. As environmental regulations are strict enough on the application of cutting fluids in industries, a new machining technique using spray impingement cooling which is near to dry machining has been studied and explored in this research of hard turning. This may improve the overall machinability aspects in hard turning and may be considered as a feasible substitute compared to dry hard finishing operation. Hard machining of AISI D2 alloy steel with low cost coated carbide tool under spray impingement cooling (SIC) environment possibly not investigated and are lacking as far as literature is concerned. Thus, extensive investigations on machinability

accomplishment of coated carbide cutting tool in turning process of AISI D2 heat-treated steel will absolutely create an avenue and beneficial for machining industries point of view to achieve their goals. This is the novelty of the present research which has been extensively investigated concerning wear at the flank face, cutting temperature, surface roughness, chip morphology, chip reduction coefficient and tool life. Furthermore, optimization, modeling, and economic aspects have also been studied in this research. This will definitely a systematic study towards its applicability in hard turning applications under SIC environment.

## 2. EXPERIMENTAL DETAILS

### 2.1 Material and Applications

A cylindrical rod of AISI D2 tool steel (high chromium and high carbon) with 48 mm diameter and 200 mm cutting length has been chosen as a test specimen for this work. The test workpiece hardness has been improved to (55±1) HRC using heat treatment process succeeded by oil quenching. Hardened D2 steel offers excellent wear and abrasion resistance, due to the presence of large quantities of carbides in the microstructure. Heat treated steel has plenty of applications in press-tool manufacture, moulds and dies manufacture, automobile, electronic industries etc. [15-16], but it is considered as a difficult to turned metal, so an investigation of optimal machining conditions for machining of D2 steel is highly needful. Hence, in the present work hardened D2 steel has been selected as work material to investigate their machinability.

### 2.2 Design and Methods

The present work utilized Taguchi $L_{16}$ orthogonal array design to conduct the turning experiments. Commercially available CVD multilayer coated (TiN/TiCN/$Al_2O_3$/TiN) carbide insert (WIDIA make) is implemented to assess the machinability of hardened AISI D2 steel under spray impingement cooling (SIC) surrounding. The insert of ISO designation CNMG120408 has approach angle of $95^0$, rake angle of $-6^0$ and nose radius of 0.8 mm respectively with application array of P15-P30. The cutting tool is firmly screwed on a tool holder of ISO designation PCLNR 2525 M12. A medium duty high precision HMT (NH22) lathe is used for finish turning operation of D2 steel. A spray impingement cooling setup furnished by Spraying Systems India Pvt. Ltd. (Bangalore, India) is utilized where air and water has been mixed in internal air blast nozzle (1/4 J series nozzle). The entire experiments have been conducted in spray impingement cooling situation with five cutting factors namely cutting speed (m/min), cutting feed (mm/rev), depth of cut (mm), air pressure (bar) and water pressure (bar). The air pressure (1.5 bars) and water pressure (1 bar) have been considered a fix for the entire set of experiments [7]. The other cutting factors like cutting speed, feed and depth of cut have four levels as reported in Table 1. HITACHI makes SU3500 Scanning electron microscope is used to capture the tool-tip SEM and EDS (Energy Dispersive Spectroscopy) analysis. In the hard turning process, L/D (length to diameter) ratio was kept to be lower than 10 using tailstock hold up (ISO standard 3685) [17].

**Table 1.** Cutting factors and their levels.

| Factors | Notation | Unit | Levels of factors | | | |
|---|---|---|---|---|---|---|
| | | | 1st | 2nd | 3rd | 4th |
| Depth of cut | *d* | mm | 0.1 | 0.2 | 0.3 | 0.4 |
| feed | *f* | mm/rev | 0.04 | 0.08 | 0.12 | 0.16 |
| Cutting speed | *v* | m/min | 63 | 108 | 140 | 182 |

The machinability measures factors like flank wear (VBc), surface roughness (Ra), chip-tool interface temperature (T), chip reduction coefficient (CRC) and chip morphology are considered for this work. Taylor Hobson (Sutronic 25) surface roughness tester has been used to quantify the average work surface roughness. The measurement for Ra has been carried on five different portions of the turned surface and its arithmetic mean has been taken as final Ra for the test sample. Chip-tool interface temperature is assessed during experimentation by a FLUKE Ti32 thermal camera as shown in Fig. 1. The thermal camera is kept at a distance of about 30 cm from the tool-work contact surface. J.B. Saedon used emissivity value 0.81 for AISI D2 steel (62 HRC) to calculate cutting temperature. However in present work, 0.81 emissivity value has been incorporated in fluke thermal camera to

measure the cutting temperature [18]. The maximum T value during each run has been considered for study. Images of flank wear, finished work surface and chip were taken by Olympus optical microscope (STM6). Finished work surface images for Flank wear width are measured using Olympus stream basic software. Chip thickness measurement for evaluating CRC has been carried using digital vernier caliper. For calculating the tool life of cutting insert, the finish turning process using optimum condition was carried out till the flank wear width (VBc) reached to 0.3 mm. This permissible wear (VBc = 0.3 mm) was set as per ISO 3685 standard (1993) and measured at nose radius corner [4, 14]. As the depth of cut is less (0.1 to 0.4 mm) compared to tip radius (0.8 mm), VBc is taken for measurement instead of $VB_b$. Minitab 16 software has been used for quadratic modeling as well as ANOVA. Schematic view of the entire work is displayed in Fig. 1. The test results are listed in Table 2.

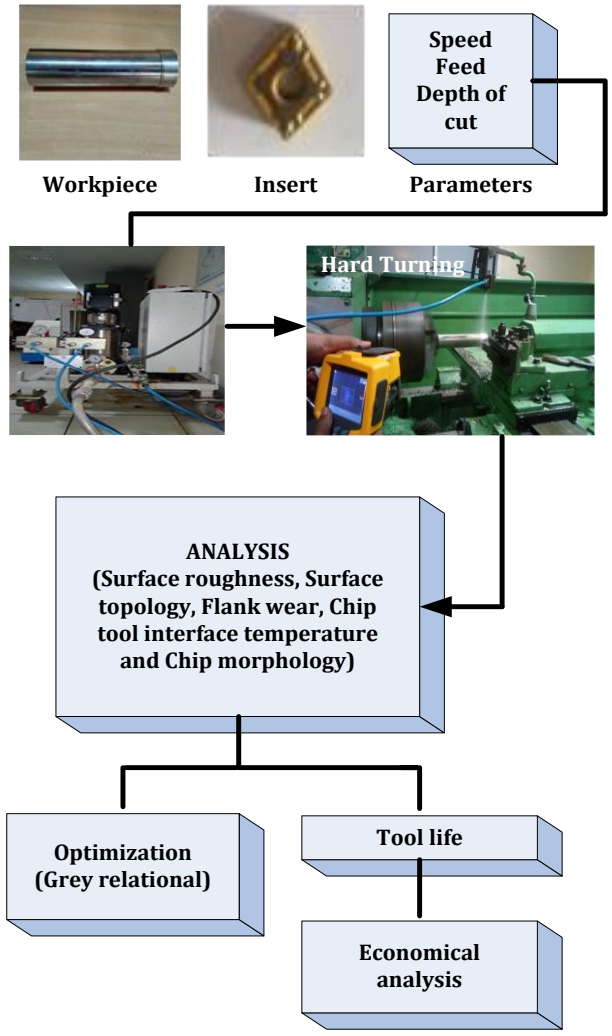


**Fig. 1.** Schematic outlines of current work.

## 3. RESULT MORPHOLOGY

### 3.1 Discussion on Aspects of Surface Roughness

The current work carried under spray impingement cooling environment where high pressure and high velocity of cutting fluid supplied which penetrates into cutting zone easily by capillary action that leads to the decline of friction between tool-chip [7]. However, in most of the turning tests, the Ra is noticed to be smaller than the recommended roughness criteria of 1.6 μm [15]. Hence for surface roughness concern, the multi-coated carbide tool performed well under the SIC machining conditions. The trend of Ra is increasing with feed while it is decreasing when cutting speed increasing to 108 m/min, thereafter improving with increasing cutting speed. It happens because of an increase in feed rate leads to the increase of heat generation thus flank wear, which attributed the rise in surface roughness. Also, machining with highest feed rate induced more chatter and attributed the incomplete machining at faster traverse as a result higher surface roughness produced. Nurhaniza et al. stated the similar reason [19]. Also, at lowest cutting speed (63 m/min) machining, there is sufficient time available to penetrate the coolant in to cutting zone, which reduces the frictions significantly thus lower intensity of heat produced which retards the tool-wear growth, as a result the perfect contact between tool-tip and workpiece established thus smooth cutting takes place which gives better surface finish. But at 108 m/min, the effect of coolant is relatively reduced as a result, more surface roughness produced. Also, beyond 108 m/min, the growth in tool wear is higher which ultimately increases the surface roughness and it is evident from the experimental results (Table 2).

Similarly, the Ra was decreasing up to 0.2 mm depth of cut while beyond it roughness value improving gradually with the depth of cut. It happens due to the following reasons: Lower depth of cut machining requires lower cutting forces to cut the material and with increasing depth of cut cutting force increases. However in current work, up to 0.2 mm of a depth of cut, lower frictions thus lower cutting forces induced due to an application of water jet, which ultimately declines the Ra and beyond it, due to the higher thickness of material removal, higher

cutting forces generated which attributed the higher Ra. Ghoreishi et al. stated that the growth in the depth of cut results in more cutting forces which increases the surface roughness [20]. Also, beyond 0.2 mm of a depth of cut, the growth in tool wear is higher which ultimately increases the surface roughness and it is evident from the experimental results (Table 2).

From 3D surface plot (Fig. 2), the surface roughness improving with rising feed and depth of cut as shown in Figs. 2a-2b. The lowest speed with the highest feed also produces higher surface roughness as shown in Fig. 2c and with improving feed and speed also attributes higher magnitudes of Ra (Fig. 2d). Similarly higher magnitudes of Ra have been seen at the lowest depth of cut with the highest speed or the lowest speed and highest depth of cut cutting scenario (Figs. 2e-2f). Overall effects of all six pair of factors are significant as rising surface roughness is noticed through the surface plot. According to ANOVA (Table 3) all the three parameters are significant and the influence of feed (48.75 % contribution) on Ra is highest [15].

**Table 2.** Test results.

| Run | ap (mm) | fn (mm/rev) | vc (m/min) | Ra (μm) | T (°C) | VBc (mm) | Chip Shape & Colour | CRC |
|---|---|---|---|---|---|---|---|---|
| 1 | 0.1 | 0.04 | 63 | 0.616 | 126.5 | 0.047 | Helical & Metallic | 1.656 |
| 2 | 0.1 | 0.08 | 108 | 0.656 | 132.8 | 0.058 | Helical & Metallic | 1.480 |
| 3 | 0.1 | 0.12 | 140 | 0.908 | 152.5 | 0.143 | Spiral c & Metallic | 1.305 |
| 4 | 0.1 | 0.16 | 182 | 1.202 | 178.9 | 0.29 | Spiral c & Burnt Blue | 1.330 |
| 5 | 0.2 | 0.04 | 108 | 0.58 | 138.7 | 0.09 | Helical & Metallic | 1.756 |
| 6 | 0.2 | 0.08 | 63 | 0.748 | 147.3 | 0.101 | Helical & Metallic | 1.631 |
| 7 | 0.2 | 0.12 | 182 | 0.996 | 198.4 | 0.465 | Spiral c and ε & Burnt blue | 1.472 |
| 8 | 0.2 | 0.16 | 140 | 0.892 | 172.4 | 0.367 | Helical & Partial blue | 1.518 |
| 9 | 0.3 | 0.04 | 140 | 0.708 | 166.6 | 0.272 | Helical & Metallic | 1.857 |
| 10 | 0.3 | 0.08 | 182 | 0.896 | 208 | 0.516 | Helical & Burnt blue | 1.807 |
| 11 | 0.3 | 0.12 | 63 | 1.036 | 152.8 | 0.181 | Ribbon & Metallic | 1.740 |
| 12 | 0.3 | 0.16 | 108 | 0.972 | 156.2 | 0.162 | Helical & Metallic | 1.669 |
| 13 | 0.4 | 0.04 | 182 | 1.036 | 200.6 | 0.52 | Spiral c & Burnt blue | 2.057 |
| 14 | 0.4 | 0.08 | 140 | 1.004 | 180.4 | 0.213 | Spiral c & Burnt blue | 1.932 |
| 15 | 0.4 | 0.12 | 108 | 1.16 | 168 | 0.112 | Ribbon & Blue | 1.991 |
| 16 | 0.4 | 0.16 | 63 | 1.376 | 148 | 0.068 | Helical & Metallic | 1.982 |

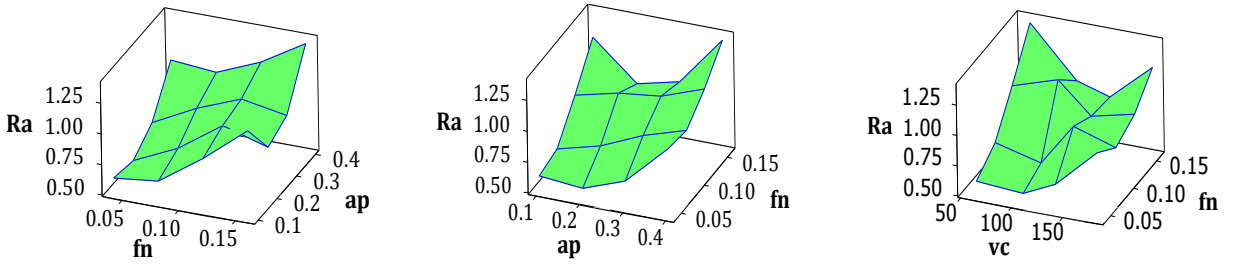


a) Surface Plot of Ra vs ap, fn

b) Surface Plot of Ra vs fn, ap

c) Surface Plot of Ra vs fn, vc

d) Surface Plot of Ra vs vc, fn

e) Surface Plot of Ra vs vc, ap

f) Surface Plot of Ra vs ap, vc

**Fig. 2.** 3-Dimensional surface plot for Ra.

**Table 3.** ANOVA results for responses Ra and VBc.

| Ra | | | | | | | | |
|---|---|---|---|---|---|---|---|---|
| **Source** | **DF** | **Seq SS** | **Adj SS** | **Adj MS** | **F** | **P** | **% contribution** | **Remarks** |
| ap | 3 | 0.27761 | 0.27761 | 0.09253 | 30.70 | 0.000 | 37.46 | Significant |
| fn | 3 | 0.36123 | 0.36123 | 0.12041 | 39.95 | 0.000 | 48.75 | Significant |
| vc | 3 | 0.08404 | 0.08404 | 0.02801 | 9.29 | 0.011 | 11.34 | Significant |
| Error | 6 | 0.01808 | 0.01808 | 0.00301 | | | 2.45 | |
| Total | 15 | 0.74098 | | | | | 100 | |
| S = 0.0549022 R² = 97.56 % R²(adj) = 93.90 % | | | | | | | | |
| **VBc** | | | | | | | | |
| ap | 3 | 0.04992 | 0.04992 | 0.01664 | 3.57 | 0.086 | 12.5 | Insignificant |
| fn | 3 | 0.00028 | 0.00028 | 0.00009 | 0.02 | 0.996 | 1.00 | Insignificant |
| vc | 3 | 0.32109 | 0.32109 | 0.10703 | 22.97 | 0.001 | 80.42 | Significant |
| Error | 6 | 0.02795 | 0.02795 | 0.00466 | | | 6.08 | |
| Total | 15 | 0.39926 | | | | | 100 | |
| S = 0.0682616 R² = 93.00% R²(adj) =82.49% | | | | | | | | |

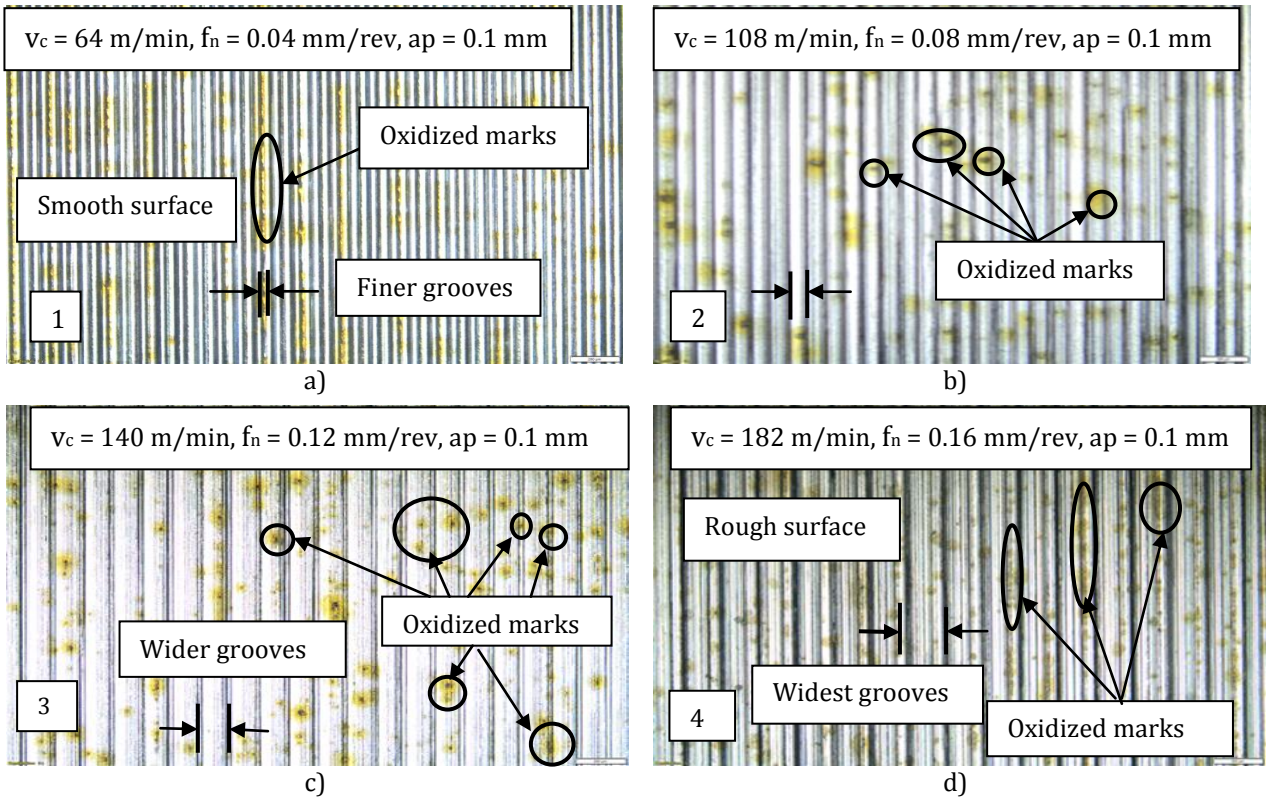


**Fig. 3.** Surface topology at different cutting conditions (Ra1 < Ra2 < Ra3 < Ra4).

### 3.2 Surface Topology of Finished Surfaces using Optical Micrographs

For material surface characterization point of view, surface topology of finished surface is required to investigate the quality of the finished surface. Presently, surface topology represented by the maximal and minimal gap between the grooves lines generated upon the machined surface due to the cutting feed. Surface topography for discrete trails (1st to 4th run) was illustrated in Fig. 3.

In Fig. 3a, very fine grooves are noticed on the machined surface which is the result of turning with the most minimal feed of (0.04 mm/rev), while in Fig. 3b, wider groove lines are seen as it was machined with little higher feed (0.08 mm/rev). Similarly in Fig. 3c, even wider grooves are noticed compared to previous cases due to its elevated feed value of 0.12 mm/rev.

The widest grooves are noticed (Fig. 3d) at highest feed (0.16 mm/rev) condition. This analysis attributes that the turning with largest feed values presents wider groves, while fine grooves are noticed with lowest feed value which attributes that the surface roughness is maximum when grooves are widest at highest feed rate and

surface roughness is in decreasing in nature with reducing gap between grooves however lowest surface roughness or highest quality of finished surface is produced with lowest feed rate where grooves are fine. With the application of spray (air-water mixture) oxidation on turned surface took place as noticed in Fig. 3. Usually, the formation of rust on to the metallic surface is called corrosion and rust is a form of iron oxide. However, if rusting or corrosive marks more on to the surface i.e. oxidation is more. From Figs. 3a-3d, the density of corrosive marks (rust) is increasing with speed and feed i.e. it may be stated that the oxidation is accelerated with speed and feed values.

### 3.3 Discussion on Aspects of Tool Flank Wear

Tool wear represents the performance and ability of the tool to cut the materials effectively and qualitatively. Cutting tool gradually wear out due to high heat and high stress developed in machining. Gradual wear is classified in two ways namely crater wear and flank wear. The progression rate of flank wear is more compare to crater wear hence in the current investigation, only flank wear is considered for tool failure analysis. The tool wear analysis has been done on recommended flank width limit of 0.3 mm [15,21].


a)

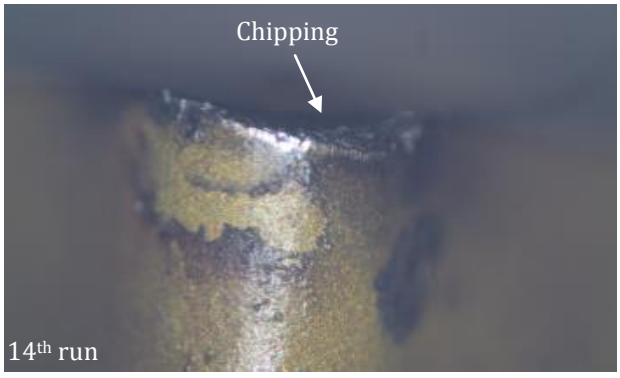


b)

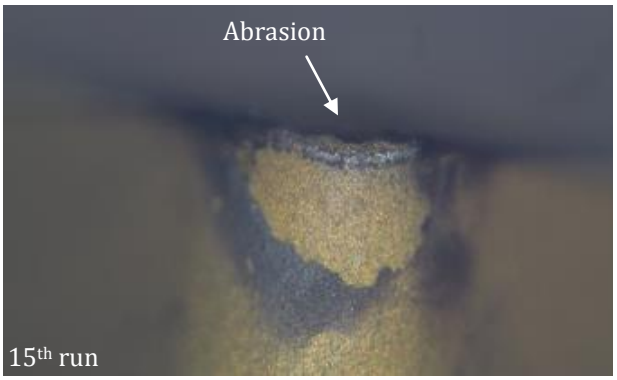


c)


d)

**Fig. 4.** Wear pattern at tool tip.

Machining under SIC reduces the friction between tool-chip which declines the rate of growth of abrasion wear. Due to the presence of water in SIC, an oxide layer is formed at the chip-tool interface which works as diffusion barricade in between chip and tool. Formation of the oxide layer depends on the quantity of oxygen and cutting speed. Inadequate amount of oxygen retards the formation of the oxide layer whereas at optimal condition a steady oxidize-layer can be generated. Below the optimal cutting speed, less amount of the oxide-layer formed and the formation of oxide layer is absent at higher cutting speed. From the turning test results (Table 2), it was identified that the flank wear is more or less lies below the standard limit of 0.3 mm flank width expect at elevated cutting speed 182 m/min due to the presence of hard lubricious, thermal barrier and wear resistant coating combinations like TiN, $Al_2O_3$ and TiCN over the carbide substrate which prevents the growth of tool wear [4]. The abrasion and chipping are seemed to be major mechanisms associated with wear (Fig. 4). At smaller cutting speeds (63 and 108 m/min) abrasion is found to be dominating wear mechanism as oxide layer is formed in between chip and tool, whereas, at higher cutting speeds

(140 and 182 m/min) more heat is generated and it is sufficient to destroy the formed oxide layer however diffusion is more dominant than abrasion and along with some abrasive marks catastrophic breakage and or chipping of tool takes place in the present study. Rubbing action in between chip-tool promotes abrasion wear whereas chipping of tool produced due to less toughness of tool, high stress and shocks produced during cutting action at a higher cutting speed, cutting feed and depth of cut. Also, abrasion is prominent due to the abrasive performance of several hard components are existing in D2 steel. Catastrophic failure of the tool developed due to the absence of diffusion barrier in between chip and tool. A high thermal shock is generated due to higher heat and high stress at a higher cutting speed, feed and depth of cut cutting situation [21].

### 3.4 EDS with SEM analysis of flank wear

SEM and EDS view and elemental composition before and after machining (7th run) has been shown in Fig. 5 respectively particularly at elevated cutting speed (182 m/min). At this elevated cutting speed, the top coatings of tool-tip layer are chipped out by catastrophic action as shown in Fig. 5.

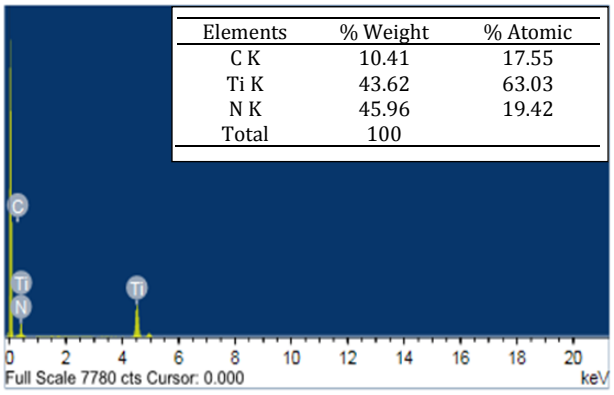


a) Before machining

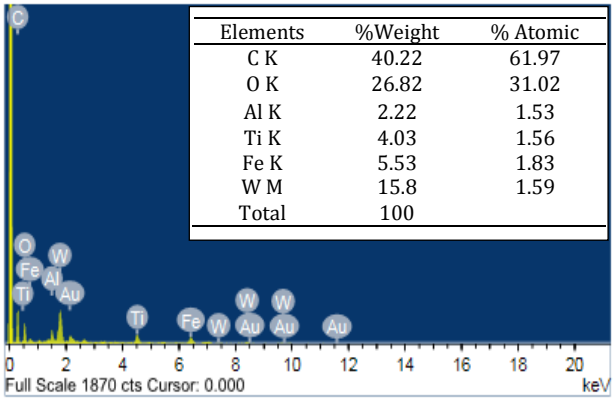


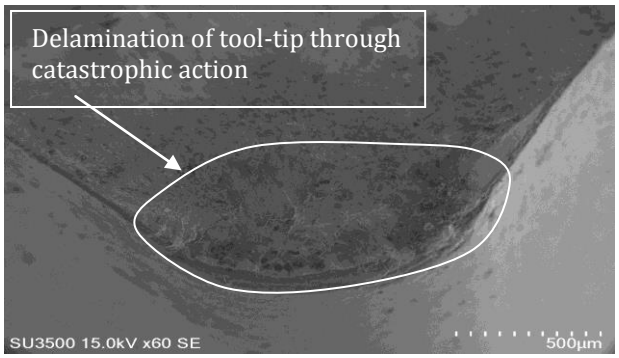


b) After machining (Run 7)

**Fig. 5.** EDS result of tool-tip with SEM image (Run7).

As a result, new elements like oxygen (O), iron (Fe), aluminum, (Al), tungsten (W) and Silver (Au) are found in EDS analysis as shown in Fig. 5. This reveals a predominant adhesive and diffusion wear mechanism that leads to catastrophic damage at elevated cutting speed range in turning of AISI D2 steel. Percentage of carbon content improves which indicates some portions of carbon content is diffused from D2 steel and adhered to the tool-tip. Presence of aluminum and oxygen indicate delamination of TiN coating in the coated carbide insert after machining and some adjacent layers may be exposed. Similarly, the presence of tungsten confirms the removal of coatings from the tip of coated carbide tools at that particular region and substrate is exposed.

Influence of feed and depth of cut on the surface plot (Fig. 6) is not prominent as surface plots are rising initially and then decline with growth in the feed as well as the depth of cut as shown Figs. 6a-b. Combine effects of feed-cutting speed and depth of cut-cutting speed are highly dominating which was ensured through elevating surface graph (Figs. 6c-6f). However, dominancy of cutting speed over flank wear is clearly seen in 3D surface plots. From ANOVA (Table 3), cutting speed is traced be a significant cutting agent for flank wear (80.42 % contribution) while feed and depth of cut are insignificant at 95 % confidence level [15,21].

### 3.5 Discussion on Aspects of Chip-Tool Interface Temperature

In turning of hardened metal, high amount of heat is engendered owing to friction action between chip-tool and tool-work interface. Generation of high cutting temperature in turning process deteriorates the quality of finish

and thus accelerates tool-tip wear. This is detrimental as far as machinability is concerned. In the dry cutting scenario, an evolution of higher heat softens the work material which makes the metal cutting easier. But at the same time, tool wear accelerates and becomes plastically deformed and thus unable to machine as the geometry of cutting tool is lost. Hence to address on this aspect, researchers are more interested to lower the cutting temperature at significant level by impinging minute amount of lubricant/coolant at tool-work interface in order to compromise between dry and wet cutting. However this research has been carried under spray impingement cooling system to study the performance of the tool which seems to be near-dry machining.

In the spray impingement application, the heat-transfer occurs due to convection as well as evaporation. The evaporation occurred due to the atomization of water particles. As the enthalpy of water is very large, evaporation of minute quantities of water droplets is sufficient enough for significant cooling as the maximum temperature has been found to be 200.6 $^0$C (Fig. 7a) and 208 $^0$C (Table 2) respectively noticed from the temperature profile for 13$^{th}$ and 10$^{th}$ run. From Figs. 7a-7d, the temperature reduces when cutting speed reduces. Also due to high pressure and high velocity of spray, air/water mixture easily penetrates at the cutting zone and facilitates more adequate cooling at the machining zone.

A significant augment in temperature with cutting speed in addition to the depth of cut has been observed (Table 2). The higher temperature is reported at higher cutting speeds (182 and 140 m/min) whereas; the variation of temperature due to varying feed is uneven. The depth of cut influencing significantly to the cutting temperature as temperature is increasing with improving the depth of cut because of the higher plastic deformation at the primary and secondary deformation region [22].

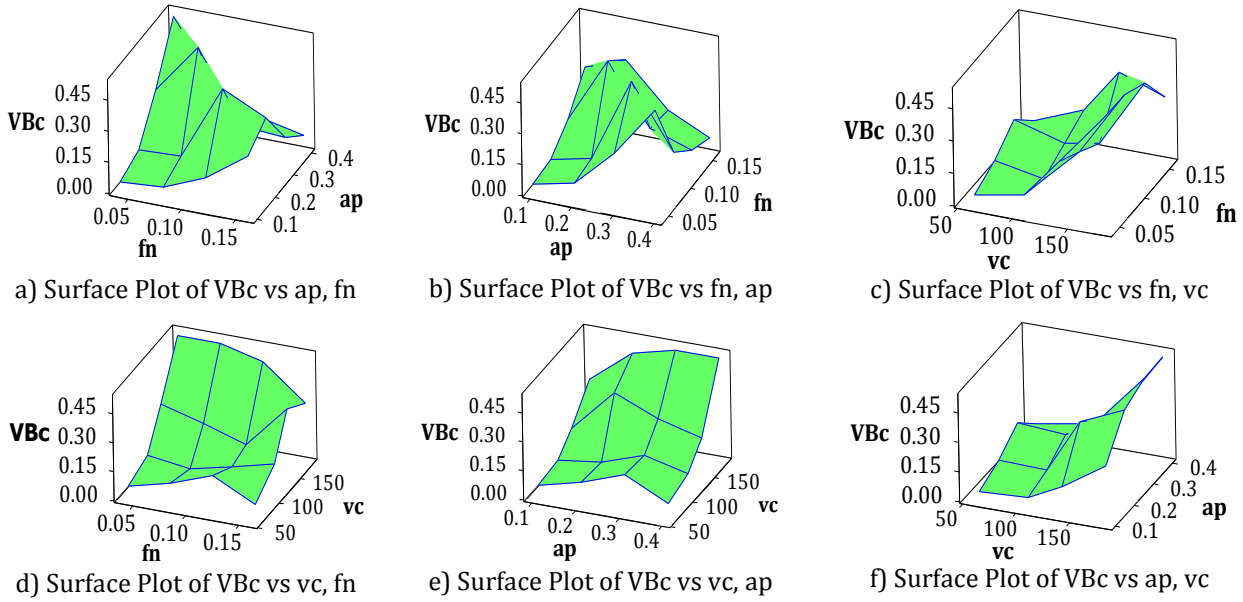


a) Surface Plot of VBc vs ap, fn
b) Surface Plot of VBc vs fn, ap
c) Surface Plot of VBc vs fn, vc
d) Surface Plot of VBc vs vc, fn
e) Surface Plot of VBc vs vc, ap
f) Surface Plot of VBc vs ap, vc

**Fig. 6.** 3-Dimensional surface plot for VBc.

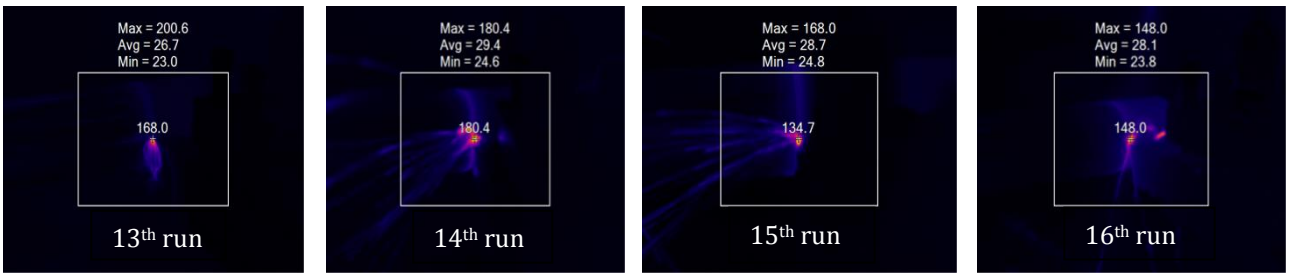


a) b) c) d)

**Fig. 7.** Infra-red thermal image of T.

**Table 4.** ANOVA results for responses T and CRC.

| T | | | | | | | | |
|---|---|---|---|---|---|---|---|---|
| **Source** | **DF** | **Seq SS** | **Adj SS** | **Adj MS** | **F** | **P** | **% contribution** | **Remarks** |
| ap | 3 | 1675.82 | 1675.82 | 558.61 | 21.70 | 0.001 | 18.8 | Significant |
| fn | 3 | 238.94 | 238.94 | 79.65 | 3.09 | 0.111 | 2.68 | Insignificant |
| vc | 3 | 6846.17 | 6846.17 | 2282.06 | 88.66 | 0.000 | 76.8 | Significant |
| Error | 6 | 154.43 | 154.43 | 25.74 | | | 1.72 | |
| Total | 15 | 8915.36 | | | | | 100 | |
| S = 5.07336 | | | $R^2$ = 98.27% | | | $R^2$(adj) = 95.67% | | |
| **CRC** | | | | | | | | |
| ap | 3 | 0.665618 | 0.665618 | 0.221873 | 91.85 | 0.000 | 81.13 | Significant |
| fn | 3 | 0.113742 | 0.113742 | 0.037914 | 15.70 | 0.003 | 13.86 | Significant |
| vc | 3 | 0.026531 | 0.026531 | 0.008844 | 3.66 | 0.083 | 3.23 | Insignificant |
| Error | 6 | 0.014494 | 0.014494 | 0.002416 | | | 1.78 | |
| Total | 15 | 0.820385 | | | | | 100 | |
| S = 0.0491492 | | | $R^2$ = 98.23% | | | $R^2$(adj) = 95.58% | | |

ANOVA (Table 4) ensured that the cutting speed (76.8 % contribution) is highly significant for temperature (T) succeeded by the depth of cut (18.8 % contribution) while the feed is irrelevant [23]. As the maximum temperature generated among all runs is 200.6 $^0$C from which it is clearly ensured that the use of air-water jet spray cooling system has the ability to reduce the chip-tool interface temperature.

From surface plot (Similar as Figs. 2 and 6), combine influence of feed-depth of cut is not relevant as surface initially elevating and then decline with feed and depth of cut whereas consequence of cutting speed-feed and cutting speed-depth of cut is more dominant as with rising in cutting speed-feed, cutting speed-depth of cut and depth of cut-cutting speed the temperature improves significantly.

### 3.6 Discussion on Chip Morphology

It is quite evident that high amount of heat is generated at the cutting zone in hard turning operations due to friction between work-tool and chip-tool interface. Due to the tangle of the chip in between tool and work surface, friction increases. The tangle of the chip depends on its shape and also major portions of heat are carried away by the chip. So, the morphology of shape and colour of chip is highly essential in hard turning operation. The categorization of different chip samples at different parametric conditions under SIC environment has been shown in Table 2 and Fig. 8 respectively.

In the present work, the shape of chips produced is either helical or ribbon or spiral c and ε type. But in maximum case, chip produced are helical in nature or spiral c type. Helical shape chips are easily eradicated from the cutting region and thus reduce friction and cutting temperature. Spiral and ribbon may be tangle between work and tool surfaces and increase friction and cutting temperature significantly. The chips colour have been found either metallic or partial blue or blue or burnt blue (Fig. 8 and Table 2).

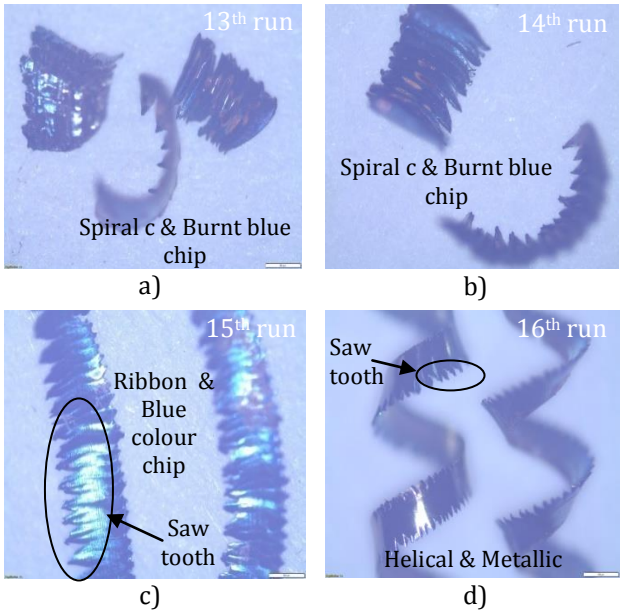


**Fig. 8.** Images of chips produced in hard turning.

The colour of chips has metallic particularly at low and moderate cutting speed range i.e. from 63-108 m/min due to the reduction of cutting temperature by spray impingement cooling. However, with higher cutting speed (140-182 m/min), chip colour is noticed to be burnt blue due to an increase of heat generation in the cutting zone. As a result, high amount of heat is

carried out through the chip which in turn gives rise to burnt blue colour shape in nature. Also, at higher cutting speed, heated chip gets quenched and the chips colour changes to partial blue (some portion of chip is blue and some portion is metallic) or blue or burnt blue. In each test run, saw tooth chips are noticed. Saw tooth chip produced due to large micro cracks formed in compressive zone and when the compressive strength is high enough to shear out the chip along the tool surface. At that instant, micro-crack is delocalize as well as distributed along the length of chip and looks like a saw tooth. Similar aspects regarding chip morphology have been reported by some researchers [4,24-26].

### 3.7 Evaluation of chip reduction coefficient

Cutting parameters sway the thickness of chip through hard turning process. The degree of thickening is called chip reduction coefficient. Chip reduction coefficient (CRC) plays a sizeable role in cutting force, power consumption as well as specific energy used in machining action and cutting temperature and considered as important indices of machinability. So, the analysis of chip reduction coefficient is highly needed for machinability point of view and less is the CRC, higher is the machinability [24].

In this work, CRC is estimated on the basis of the ratio of the measured thickness of chip to the before cut chip thickness. The experimental result reveals the value of CRC lies in between 1.305-2.057 which is quite less and is an indication of favorable machining under spray impingement cooling (Table 2). Reduction of CRC also implies the reduction of cutting temperature and chip-tool interface friction during hard turning. Chip reduction coefficient increases with an increase of depth of cut while it declines with increasing cutting speed and feed. Highest CRC value has been observed at $13^{th}$ run i.e. at the highest depth of cut (0.4 mm), highest cutting speed (182 m/min) and lowest feed (0.04 mm/rev). At these parametric conditions, higher machining force is expected to be generated as well as higher power consumption during cutting action and this attributes to the reduction in machinability. Interestingly, the experimental observation seems to be very adverse at this parametric conditions i.e. Ra, T, and VBc are found to be 1.036 μm, 200.6 $^0$C and 0.52 mm respectively and also spiral C-type with saw-tooth and burnt blue colour chips obtained. It is evident that higher temperature generated which in turn flank wear beyond the criteria of 0.3 mm.

From surface plot (Similar as Figs. 2 and 6), the CRC is increasing with improving the depth of cut while it is reducing with improving cutting speed and cutting feed. The surface gets decline and attained the lowest CRC at highest feed and lowest depth of cut conditions whereas the CRC surface gets rising with improving the depth of cut and reducing feed. In other surface plots, it can visualize that the 3D surface gets deteriorate with cutting speed as well as the depth of cut while combine the effects of speed and feed are not relevant. From ANOVA (Table 4), depth of cut is the highest influencing cutting inputs for CRC (81.13 % contribution) succeeded by feed (13.86 % contribution) while cutting speed is traced to be insignificant at 95 % of the level of confidence [23-26].

## 4. MULTI-RESPONSE OPTIMIZATION

In the present work, Taguchi based grey relational analysis approach is implemented to evaluate parametric optimization of multi responses as referred [6,15,24,27-29]. Taguchi $L_{16}$ is selected for conducting the turning runs and the results are reported in Table 2. The experimental data have been normalized for all responses considering lower the better criteria for surface roughness (Ra), chip-tool interface temperature (T) and flank wear (VBc) respectively called grey relational generation and shown in Table 5. Grey relation coefficient (GRC) with equal weight ($\phi$=0.5), grey relational grade (GRG) and their rank are calculated and presented in Table 5. The stepwise sample calculation of grey relational generation, GRC, and GRG for Run 1 is mentioned in Appendix. Mean grey relational grade of output responses is described in Table 6. From Table 6, highest mean grey relational grade of respective parameters indicates the optimal set of input cutting variables and the optimum setting of factors are $ap_1$-$fn_1$-$Vc_2$ i.e. depth of cut = 0.1 mm, feed rate = 0.04 mm/rev and cutting speed = 108 m/min correspondingly. Cutting speed is traced to be the most dominant input term for multi-responses in hard turning operation as evident from the highest rank (0.317) of Table 6.

**Table 5.** Stepwise calculation for GRG.

| Run No. | Calculation of GRGen | | | Calculation of Δoi | | | Calculation of GRC | | | GRG | Rank |
|---|---|---|---|---|---|---|---|---|---|---|---|
| | Ra | T | VBc | Ra | T | VBc | Ra | T | VBc | | |
| Ideal sequence | 1.000 | 1.000 | 1.000 | 0.000 | 0.000 | 0.000 | 1.000 | 1.000 | 1.000 | | |
| 1 | 0.955 | 1.000 | 1.000 | 0.045 | 0.000 | 0.000 | 0.917 | 1.000 | 1.000 | 0.972 | 1 |
| 2 | 0.905 | 0.923 | 0.977 | 0.095 | 0.077 | 0.023 | 0.840 | 0.866 | 0.956 | 0.887 | 2 |
| 3 | 0.588 | 0.681 | 0.797 | 0.412 | 0.319 | 0.203 | 0.548 | 0.610 | 0.711 | 0.623 | 6 |
| 4 | 0.219 | 0.357 | 0.486 | 0.781 | 0.643 | 0.514 | 0.390 | 0.437 | 0.493 | 0.440 | 13 |
| 5 | 1.000 | 0.850 | 0.909 | 0.000 | 0.150 | 0.091 | 1.000 | 0.770 | 0.846 | 0.872 | 3 |
| 6 | 0.789 | 0.745 | 0.886 | 0.211 | 0.255 | 0.114 | 0.703 | 0.662 | 0.814 | 0.726 | 4 |
| 7 | 0.477 | 0.118 | 0.116 | 0.523 | 0.882 | 0.884 | 0.489 | 0.362 | 0.361 | 0.404 | 15 |
| 8 | 0.608 | 0.437 | 0.323 | 0.392 | 0.563 | 0.677 | 0.561 | 0.470 | 0.425 | 0.485 | 12 |
| 9 | 0.839 | 0.508 | 0.524 | 0.161 | 0.492 | 0.476 | 0.757 | 0.504 | 0.512 | 0.591 | 7 |
| 10 | 0.603 | 0.000 | 0.008 | 0.397 | 1.000 | 0.992 | 0.557 | 0.333 | 0.335 | 0.409 | 14 |
| 11 | 0.427 | 0.677 | 0.717 | 0.573 | 0.323 | 0.283 | 0.466 | 0.608 | 0.638 | 0.571 | 9 |
| 12 | 0.508 | 0.636 | 0.757 | 0.492 | 0.364 | 0.243 | 0.504 | 0.578 | 0.673 | 0.585 | 8 |
| 13 | 0.427 | 0.091 | 0.000 | 0.573 | 0.909 | 1.000 | 0.466 | 0.355 | 0.333 | 0.385 | 16 |
| 14 | 0.467 | 0.339 | 0.649 | 0.533 | 0.661 | 0.351 | 0.484 | 0.431 | 0.588 | 0.501 | 11 |
| 15 | 0.271 | 0.491 | 0.863 | 0.729 | 0.509 | 0.137 | 0.407 | 0.495 | 0.784 | 0.562 | 10 |
| 16 | 0.000 | 0.736 | 0.956 | 1.000 | 0.264 | 0.044 | 0.333 | 0.655 | 0.918 | 0.635 | 5 |

**Table 6.** Estimation of mean grey relational grade.

| Factors | Mean grey relational grade | | | | Maximum – Minimum | Rank |
|---|---|---|---|---|---|---|
| | 1st level | 2nd level | 3rd level | 4th level | | |
| ap | 0.731 | 0.622 | 0.539 | 0.521 | 0.210 | 2 |
| fn | 0.705 | 0.631 | 0.540 | 0.537 | 0.168 | 3 |
| Vc | 0.726 | 0.727 | 0.550 | 0.409 | 0.317 | 1 |

The rank has been calculated as the difference of the maximum and minimum value of mean grey relational grade. The sequence orders of significant cutting parameters on multi-responses are cutting speed, depth of cut and lastly feed.

**Table 7.** Confirmation test result.

| Responses | Initial parameter setting $ap_2$- $fn_3$-$vc_4$ | Optimal parameter factors $ap_1$- $fn_1$-$vc_2$ |
|---|---|---|
| Ra (μm) | 0.996 | 0.636 |
| T ($^0$C) | 198.4 | 134.0 |
| VBc (mm) | 0.465 | 0.071 |
| GRG | 0.404 | 0.876 |
| Gain in GRG | 0.472 | |

The confirmation turning test is performed among initial and optimal factors as presented in Table 7. The improvements of grey relational grade are noticed as 0.472 i.e. about 116.8 % increment from initial setting is found through this approach.

## 5. TOOL LIFE ESTIMATION AND COST ANALYSIS

The tool life under air-water jet spray impingement cooling surrounding has been assessed through machining with sequential time intervals on the basis of 0.3 mm flank wear width criterion at the optimal run ($v_c$ = 108 m/min, $f_n$ = 0.04 mm/rev and $a_p$ = 0.1 mm). In the first seven minutes of machining, abrasion took place due to hard particles present in the D2 steel and due to rubbing action between tool and workpiece whereas after seven minutes, abrasion and chipping types of wear identified on the flank surface due to excessive stress and temperature (Fig. 9). The wear width has been gradually increased with the progress of machining time and the measured tool life is found as about 20.3 minutes as shown in Fig. 9. The principal target of any manufacturer is to minimize the machining cost in order to achieve a higher profit rate without compromising the quality of the product.

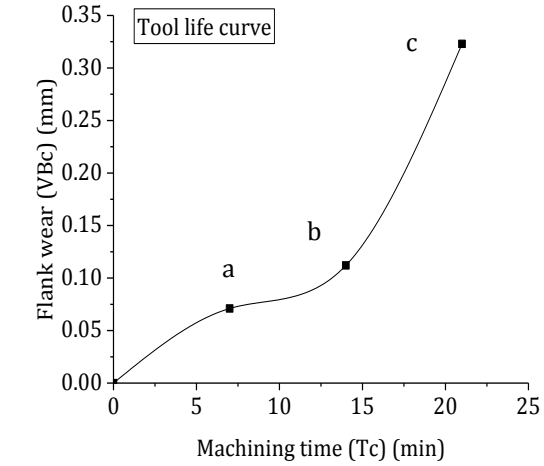


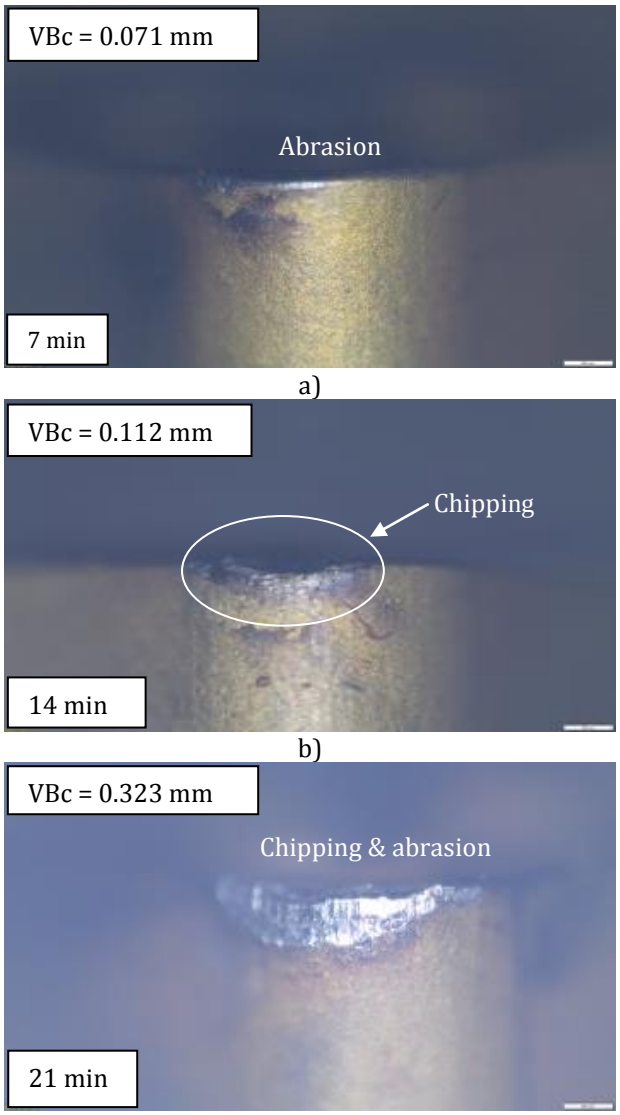


**Fig. 9.** Progress in VBc with Tc during tool life estimation.

The tool having smaller tool life causes higher tooling cost and tool changing/indexing cost. Tool life greatly depends on the mode of tool wear and magnitudes of cutting variables. So for greater tool life, the cutting parameter should be taken as smaller in magnitude but by taking the lower magnitude of cutting parameters, productivity will decline and thus machining cost increases. Hence, to establish an appropriate balance among these conflicting natures, a comprehensive cost study is highly vital in hard machining.

**Table 8.** Cost analysis.

| Steps | Cost elements | Amount |
|---|---|---|
| 1 | Lathe, cooling system and machinist cost (m), Rs 1000/ hr | Rs 16.67/min |
| 2 | Machining time (Tc) | 2.91 min |
| 3 | Machining cost in one cut (m.Tc) | Rs 48.51 |
| 4 | Tool life of one tool-tip (Tl) | 20.3 min |
| 5 | Tool interchanging cost in one cut [m Ti (Tc / Tl)] | Rs 11.95 |
| 6 | Cost of each tool-tip (n) | Rs 61 |
| 7 | Cutting tool cost in one cut [n (Tc/Tl)] | Rs 8.74 |
| 8 | Total machining cost in one cut (c), (3 + 5+ 7) | Rs 69.2 |

To evaluate the cost analysis, the tool life (Tl) is essential at optimum cutting settings and found as 20.3 min. By using Gilbert's approach [15,17,29], the total machining cost in one cut has been evaluated as shown in Table 8. The cost in one cut has been calculated taking 40 mm of initial diameter (D), 100 mm of cutting length (L), AISI D2 steel work-piece of hardness 55±1 HRC and at their optimal cutting levels correspondingly.

The ideal time (Ti) in between two consecutive full run is 5 min. The complete cost linked with Lathe, cooling system and machinist (m) is considered as Rs 1000/hour. The cost of each insert is Rs 243 and each insert has four usable tips. Henceforth, the cost of each tool-tip (n) is Rs 61. The total machining cost in one cut is calculated as Rs 69.2 and observed to be quite less. Thus, effective and economical machining has been achieved using multi-coated carbide cutting tools for hardened AISI D2 steel at the optimal parametric level under spray impingement cooling environment.

## 6. CONCLUSIONS

Hard machining using CVD coated carbide insert (TiN/TiCN/$Al_2O_3$/TiN) under SIC environment induced favorable machining that reduces the rate of growth of abrasion wear due to presence of hard lubricious thermal

barrier coatings over carbide substrate. Due to the presence of water in SIC, surface hardening of work surface produced which may improve cutting force and vibration but at the same time due to spraying form of water temperature at cutting zone reduces and an oxide layer is induced at the chip-tool interact zone which works as diffusion barrier in between chip and tool which attributes lower growth of flank wear which is confirmed as flank wear noticed within the recommended limit of 0.3 mm expect at largest chosen cutting speed of 182 m/min. Arithmetic surface roughness values are observed within the recommended limit of 1.6 microns and can be comparable with cylindrical grinding. Hence, for surface roughness concern, multi-coated carbide tool performed well under the SIC machining conditions. Feed and depth of cut are found to be the most dominant cutting factors for surface roughness trailed by cutting speed. Due to high pressure and high velocity of the water jet, the cutting fluid easily penetrates (due to capillary phenomena) into the cutting zone which facilitates more efficient cooling thus reduction in temperature. Cutting speed is highly significant for chip-tool interface temperature trailed by the depth of cut while feed rate is insignificant. Saw-tooth chips are produced as a result of large micro-cracks formed in the compressive zone. Spray impingement cooling has a positive impact on chip control thus quite less CRC (1.305-2.057) is found. The depth of cut is the highest dominant input variable for CRC succeeded by feed whereas, cutting speed is irrelevant. Tool wear successively increases with machining time and the measured tool life is found as about 20.3 minutes at optimal parametric conditions i.e. $ap_1$-$fn_1$-$vc_2$ (depth of cut-0.1 mm, cutting feed-0.04 mm/rev and cutting speed-108 m/min respectively. Total machining cost is observed to be quite less (Rs 69.2) and thus can be considered as effective and economical machining using multi-coated carbide tools for hardened AISI D2 steel (55±1 HRC) at optimal parametric conditions under spray impingement cooling environment.

## Acknowledgement

The authors would like to thank KIIT Deemed to be University, India to carry out the research work.

## REFERENCES

[1] S. Chinchanikar, S.K. Choudhury, *Investigations on machinability aspects of hardened AISI 4340 steel at different levels of hardness using coated carbide tools*, International Journal of Refractory Metals and Hard Materials, vol. 38, pp. 124-133, 2013, doi: 10.1016/j.ijrmhm.2013.01.013

[2] K. Gangatharan, N. Selvakumar, P. Narayanasamy, G. Bhavesh, *Mechanical analysis and high temperature wear behavior of AlCrN/DLC coated titanium alloy*, International Journal of Surface Science and Engineering, vol. 10, no. 1, pp. 27-40, 2016, doi: 10.1504/IJSURFSE.2016.075315

[3] Q. Gao, Y. Niu, F. Qu, Y. Wang, *Interfacial reaction and friction properties of Fe-based TiC composite coating*, International Journal of Surface Science and Engineering, vol. 10, no. 1, pp.1-10, 2016, doi: 10.1504/IJSURFSE.2016.075313

[4] A.K. Sahoo, B. Sahoo, *Performance studies of multilayer hard surface coatings (TiN/TiCN/$Al_2O_3$/TiN) of indexable carbide inserts in hard machining: Part-I (An experimental approach),* Measurement, vol. 46, iss. 8, pp. 2854-2867, 2013, doi: 10.1016/j.measurement.2013.03.04

[5] S. Chinchanikar, S.K. Choudhury, *Hard turning using HiPIMS-coated carbide tools: wear behavior under dry and minimum quantity lubrication (MQL),* Measurement, vol. 55, pp. 536-548, 2014, doi: 10.1016/j.measurement.2014.06.02

[6] A.K. Sahoo, B. Sahoo, *Performance studies of multilayer hard surface coatings (TiN/TiCN/$Al_2O_3$//TiN) of indexable carbide inserts in hard machining: Part-II (RSM, grey relational and techno economical approach),* Measurement, vol. 46, iss. 8, pp. 2868-2884, 2013, doi: 10.1016/j.measurement.2012.09.03

[7] S.K. Sahu, P.C. Mishra, K. Orra, A.K. Sahoo, *Performance assessment in hard turning of AISI 1015 steel under spray impingement cooling and dry environment,* Proceedings of IMECHE Part B: Journal of Engineering Manufacture, vol. 229, no. 2, pp. 251-265, 2015, doi: 10.1177/0954405414528165

[8] P.C. Mishra, D.K. Das, M Ukamanal, B.C. Routara, A.K. Sahoo, *Multi-response optimization of process parameters using Taguchi method and grey relational analysis during turning AA 7075/SiC composite in dry and spray cooling environments*, International Journal of Industrial Engineering Computations, vol. 6, no. 4, pp. 445-456, 2015, doi: 10.5267/j.ijiec.2015.6.002

[9] J. Sharma, B.S. Sidhu, *Investigation of effects of dry and near dry machining on AISI D2 steel using vegetable oil,* Journal of Cleaner Production, vol. 66, pp. 619-623, 2014, doi: 10.1016/j.jclepro.2013.11.042

[10] G.K. Dosbaeva, M.A.El. Hakim, M.A. Shalaby, J.E. Krzanowski, S.C. Veldhuis, *Cutting temperature effect on PCBN and CVD coated carbide tools in hard turning of D2 tool steel*, International Journal of Refractory Metals and Hard Materials, vol. 50, pp. 1-8, 2015, doi: 10.1016/j.ijrmhm.2014.11.001

[11] A. Agrawal, S. Goel, W.B. Rashid, M. Price, *Prediction of surface roughness during hard turning of AISI 4340 steel (69 HRC),* Applied Soft Computing, vol. 30, pp. 279-286, 2015, doi: 10.1016/j.asoc.2015.01.059

[12] K. Bouacha, M.A. Yallese, S. Khamel, S. Belhadi, *Analysis and optimization of hard turning operation using cubic boron nitride tool,* International Journal of Refractory Metals and Hard Materials, vol. 45, pp. 160-178, 2014, doi: 10.1016/j.ijrmhm.2014.04.014

[13] G. Bartarya, S.K. Choudhury, *Influence of machining parameters on forces and surface roughness during finish hard turning of EN 31 steel*, Proceedings of IMECHE Part B: Journal of Engineering Manufacture, vol. 228, no. 9, pp. 1068-1080, 2013, doi: 10.1177/0954405413500492

[14] H. Aouici, M.A. Yalles, K. Chaoui, T. Mabrouki, J.F. Rigal, *Analysis of surface roughness and cutting force components in hard turning with CBN tool: Prediction model and cutting conditions optimization*, Measurement, vol. 45, iss. 3, pp. 344-353, 2012, doi: 10.1016/j.measurement.2011.11.011

[15] R. Kumar, A.K. Sahoo, P.C. Mishra, R.K. Das, *An investigation to study the wear characteristics and comparative performance of cutting inserts during hard turning,* vol. 20, no. 4, 2018, doi: 10.1504/IJMMM.2018.094730

[16] K. Orra, S.K. Choudhury, *Development of flank wear model of cutting tool by using adaptive feedback linear control system on machining AISI D2 steel and AISI 4340 steel*, Mechanical Systems and Signal Processing, vol. 81, pp. 475–492, 2016, doi: 10.1016/j.ymssp.2016.03.011

[17] A.S. More, W Jiang, W.D. Brown, A.P. Malshe, *Tool wear and machining performance of cBN-TiN coated carbide inserts and PCBN compact inserts in turning AISI 4340 hardened steel*, Journal of Materials Processing Technology, vol. 180, iss. 1-3, pp. 253-262, 2006, doi: 10.1016/j.jmatprotec.2006.06.013

[18] J.B. Saedon, *Micromilling of Hardened (62 HRC) AISI D2 Cold Work Tool Steel*, PhD thesis, University of Birmingham, UK, 2012.

[19] M. Nurhaniza, M.K.A.M. Ariffin, F. Mustapha, B.T.H.T. Baharudin, *Analyzing the Effect of Machining Parameters Setting to the Surface Roughness during End Milling of CFRP-Aluminium Composite Laminates.* International Journal of Manufacturing Engineering, vol. 2016, Article ID 4680380, p. 9, 2016, doi: 10.1155/2016/4680380

[20] R. Ghoreishi, A.H. Roohi, A.D. Ghadikolaei, *Analysis of the influence of cutting parameters on surface roughness and cutting forces in high speed face milling of Al/SiC MMC*, Materials Research Express, vol. 5, no. 8, 2018, doi: 10.1088/2053-1591/aad164

[21] R. Kumar, A.K. Sahoo, P.C. Mishra, R.K. Das, *Comparative Investigation towards machinability improvement in hard turning using coated and uncoated carbide inserts: part I experimental investigation*, Advances in Manufacturing, vol. 6, iss. 1, pp. 52–70, 2018, doi: 10.1007/s40436-018-0215-z

[22] M.A. Kiprawi, A. Yassin, S.T.S. Shazali, M.S. Islam, M.A.M. Said, *Study of cutting edge temperature and cutting force of end mill tool in high speed machining*, in: MATEC Web of Conferences 87, 02030, p. 5, 2017, doi: 10.1051/matecconf/20178702030

[23] Y. Tamerabet, M. Briou, M. Tamerabet, S. Khoualdi, *Experimental Investigation on Tool Wear Behavior and Cutting Temperature during Dry Machining of Carbon Steel SAE 1030 Using KC810 and KC910 Coated Inserts*, Tribology in Industry, vol. 40, no. 1, pp. 52-65, 2018, doi: 10.24874/ti.2018.40.01.04

[24] R. Kumar, A.K. Sahoo, P.C. Mishra, R.K. Das, M. Ukamanal, *Experimental investigation on hard turning using mixed ceramic insert under accelerated cooling environment*, International journal of Industrial Engineering Computation, vol. 9, pp. 509-522, 2018, doi: 10.5267/j.ijiec.2017.11.002

[25] R. Kumar, A.K. Sahoo, P.C. Mishra, R.K. Das, *Measurement and machinability study under environmentally conscious spray impingement cooling assisted machining,* Measurement, vol. 135, pp. 913-927, 2019, doi: 10.1016/j.measurement.2018.12.037

[26] A. Das, A. Mukhopadhyay, S.K. Patel, B.B. Biswal, *Comparative Assessment of machinability aspects of AISI 4340 alloy steel using uncoated carbide and coated cermet inserts during hard turning*, Arabian Jounal for Science and Engineering, vol. 41, iss. 11, pp. 4531-4552, 2016, doi: 10.1007/s13369-016-2160-0

[27] A. Panda, A.K. Sahoo, I. Panigrahi, A.K. Rout, *Investigating machinability in hard turning of AISI 52100 bearing steel through performance measurement: QR, ANN and GRA Study,*

*International*, Journal of Automotive and Mechanical Engineering, vol. 15, iss. 1, pp. 4935–4961, 2018, doi: 10.15282/ijame.15.1.2018.5.0384

[28] M. Mia, A. Rifat, Md.F. Tanvir, M.K. Gupta, Md.J. Hossain, A. Goswami, *Multi-objective optimization of chip-tool interaction parameters using Grey-Taguchi method in MQL-assisted turning,* Measurement, vol. 129, pp. 156-166, 2018, doi: 10.1016/j.measurement.2018.07.04

[29] R. Kumar, A.K. Sahoo, P.C. Mishra, R.K. Das, *Comparative investigation towards machinability improvement in hard turning using coated and uncoated carbide inserts: part II modeling, multi-response optimization, tool life, and economic aspects*, Advances in Manufacturing, vol. 6, iss. 2, pp. 155-175, 2018, doi: 10.1007/s40436-018-0214-0

## Nomenclature

| | |
|---|---|
| ap | depth of cut (mm) |
| fn | feed rate (mm/rev) |
| vc | cutting velocity (m/min) |
| Ra | surface roughness (μm) |
| VBc | flank wear (mm) |
| T | chip-tool interface temperature ($^0$C) |
| CRC | chip reduction coefficient |
| SIC | spray impingement cooling |
| AISI | american Iron and Steel Institute |
| HRC | rockwell hardness |
| SEM | scanning electron microscope |
| EDX | energy dispersive x-ray |
| CVD | chemical vapour deposition |
| CBN | cubic boron nitride |
| ANOVA | analysis of variance |
| DF | degrees of freedom |
| SS | sum of squares |
| MS | mean square |
| F | variance ratio |
| P | probability of significance |
| $R^2$ | Coefficient of determination |
| $R^2$(pred) | predicted R2 |
| $R^2$(adj) | adjusted R2 |
| GRC | grey relational generation |
| GRG | grey relational grade |
| Tc | machining time (min) |
| Ti | idle time (min) |
| Tl | tool life of one tool-tip (min) |
| n | cost of each tool-tip (Rs) |
| C | total machining cost (Rs) |

## Appendix

Procedure and step wise sample calculation of grey relational generation, GRC and GRG.

| Steps | Sample calculation of Run1 |
|---|---|
| 1<br>Grey relational generation | $Z_i(j)=\dfrac{\max(Y_i(j))-Y_i(j)}{\max(Y_i(j))-\min(Y_i(j))}$<br>$=\dfrac{1.376-0.616}{1.376-0.580}=0.955 for Ra$<br>$=\dfrac{208-126.5}{208-126.5}=1 for T$<br>$=\dfrac{0.520-0.047}{0.520-0.047}=1 for VBc$ |
| 2 | $\Delta_{0i}=Z_0(j)-Z_i(m)$<br>$=1-0.955=0.045 for Ra$<br>$=1-1=0 for T$<br>$=1-1=0 for VBc$ |
| 3<br>Grey relational Coefficient (GRC) | $\delta_i(j)=\dfrac{\Delta_{\min}+\phi_{\max}}{\Delta_{0i}(j)+\phi\Delta_{\max}}$<br>$=\dfrac{0+0.5}{0.045+0.5}=0.917 for Ra$<br>$=\dfrac{0+0.5}{0+0.5}=1 for T$<br>$=\dfrac{0+0.5}{0+0.5}=1 for VBc$ |
| 4<br>Grey relational grade (GRG) | $\lambda_n=\dfrac{1}{n}\sum_{j=1}^{n}\delta_i(j)$<br>$=(0.917+1+1)/3=0.972$ |

Where, $Z_{ij}$ is the grey relation generation value, max ($Y_i$(j)) denotes the maximum value of ($Y_i$(j)) for the j$^{th}$ output, and min($Y_i$(j)) is the lowermost value of $Y_i$(j) for the j$^{th}$ output. $Y_i$(j) shows the reference sequence, where $j$= 1, 2, 3 (outputs). ($\Delta_{0i}$) is the absolute difference value between $Z_0(j)$ and $Z_i(J)$ and indicate the smallest and largest absolute differences value of all sequences respectively and $\phi$ = 0.5 is distinguishing coefficient. $\lambda_n$ denotes the grey relational grade (GRG)and it is the average value of the grey relational coefficient corresponding to the output responses.